



## A multi analytical characterization of a small bronze figurine from *Gran Carro* site (Bolsena Lake, Italy)

Marta Porcaro <sup>a</sup>, Barbara Barbaro <sup>b</sup>, Caterina Canovaro <sup>c,\*</sup>, Gilberto Artioli <sup>c</sup>, Chiara Lucarelli <sup>c</sup>, Federico Lugli <sup>d,e,f</sup>, Anna Depalmas <sup>g</sup>, Antonio Brunetti <sup>h</sup>

<sup>a</sup> Department of the Earth Sciences, University “La Sapienza” of Rome, Italy

<sup>b</sup> Soprintendenza Archeologia Belle Arti e Paesaggio per la provincia di Viterbo e per l'Etruria meridionale, Italy

<sup>c</sup> Department of Geosciences, University of Padova, Italy

<sup>d</sup> Department of Chemical and Geological Sciences, University of Modena and Reggio Emilia, Italy

<sup>e</sup> Department of Cultural Heritage, University of Bologna, Italy

<sup>f</sup> Institut für Geowissenschaften, Goethe University Frankfurt, Frankfurt am Main, Germany

<sup>g</sup> DUMAS Department, University of Sassari, Italy

<sup>h</sup> Biomedical Sciences Department, University of Sassari, Italy

### ARTICLE INFO

#### Keywords:

Nuragic metallurgy  
Archaeometry  
Isotopic analyses  
ED-XRF  
Monte Carlo simulations

### ABSTRACT

This paper presents the results of an archaeometric analysis carried out on an early Iron Age anthropomorphic figurine discovered in the area of the *Gran Carro* on Bolsena Lake (Latium, Italy) site, currently interpreted as a place of worship. This statuette is considered a *unicum*, both because of the context in which it was found and because of its stylistic characteristics similar to those of bronzes from the Nuragic civilization (Sardinia, Italy). Its discovery and the data obtained from this work provide further evidence in support of numerous previous studies suggesting the presence of trade and direct exchanges between Sardinia and southern Etruria. The research was performed through some non-destructive investigations such as Energy Dispersive X-Ray Fluorescence (EDXRF) combined with Monte Carlo Simulation (MC) and micro-invasive investigations such as Scanning Electron Microscopy coupled by Energy Dispersive Spectroscopy (SEM-EDS) and by Electron Probe Micro-Analysis (EPMA), metallography and lead isotope analyses (LIA), performed on a selected micro-fragment. The combination of non-destructive techniques (EDXRF-MCS) for the characterization of the artefact allowed us to obtain data similar to those obtained with micro-invasive surveys, further demonstrating the effectiveness of the method. The results indicate that the statuette is made of a bronze alloy and that the copper metal was extracted from Sardinian deposits.

### 1. Introduction

The submerged site of the “Gran Carro” on Lake Bolsena, discovered in 1959, is considered one of the best-preserved protohistoric sites in central Italy. It is located about one hundred meters from the present shore, it has been researched several times until now. The settlement is characterized by the presence of a pile-dwelling area dated to the early Iron Age and a monumental elliptical stone structure called the “Aiola” (Fig. 1).

In recent years, research has been directed by the “Servizio di Archeologia Subacquea della Soprintendenza Archeologia Belle Arti e Paesaggio per la provincia di Viterbo e per l'Etruria meridionale” with the technical support of specialized divers from the “Centro Ricerche

Archeologia Subacquea del Lago di Bolsena”.

The excavations have clarified some fundamental aspects such as the formation of the deposit, the succession of construction phases, and the intended use but especially the extent of the site and its chronology.

In the first sixty years, until 2019, investigations focused on the area where the wooden poles of the piles dwelling have surfaced (Fioravanti and Camerini, 1977; Tamburini, 1995). In 2020 it was discovered that the archaeological site also included other areas, both in the submerged area and in the currently dry area, covering an area of more than 1.5 ha. This fact also made it clear that the period of occupation of the site was much longer, it was present as early as the beginning of the Middle Bronze Age (15th cent. B.C.), until the Early Iron 2 Age (8th cent. B.C.), and in some areas such as the “Aiola” even until the 5th cent. B.C.

\* Corresponding author at: Dipartimento di Geoscienze Università di Padova, via Gradenigo 6, 35131 Padova, Italy.

E-mail address: [caterina.canovaro@unipd.it](mailto:caterina.canovaro@unipd.it) (C. Canovaro).

<https://doi.org/10.1016/j.jasrep.2023.104230>

Received 9 February 2023; Received in revised form 14 September 2023; Accepted 26 September 2023

Available online 30 September 2023

2352-409X/© 2023 The Authors. Published by Elsevier Ltd. This is an open access article under the CC BY-NC-ND license (<http://creativecommons.org/licenses/by-nc-nd/4.0/>).

(Barbaro and Severi, 2020; Barbaro, 2021).

Through stratigraphic excavations in the Aiola area, it was possible to interpret the area as a place of worship. The presence of hot springs may have determined the choice of the site, at the time not submerged by water, to be dedicated to probably chthonic deities. Its continuative use as a religious site is testified by a large amount of stones used to cover the ceremonial fires, food, and cereals, pots (both at real size as well as miniaturized), metallic objects (rings, fibulas, pins, etc), glass beads, all of them apparently ascribable - on typological basis and associations - to female individuals. Moreover, there is evidence of pots covered by plates with stones, containing remains of burned food or vegetables, which can be connected to incinerating rituals sometimes found in tombs of the same Villanovan horizon such as, for example, some from the Villa Bruschi Falgari necropolis in Tarquinia (Trucco, 2006).

Among the excavated artifacts, a small but well-defined anthropomorphic figure has been found, associated with early Iron Age objects, although its function appears to be unknown. It was possibly part of a more complex and structured object.

The figure appears to be slightly deformed, possibly due to the weight of the stones it was covered with. Several features of its complex form recall details of Sardinian bronze figurines (Sardinia, Italy) (Lilliu, 1966; Gonzalez, 2012; Moravetti et al., 2014), such as the big eyes or the braids on the back of the head (Fig. 2). This finding can be interpreted as unique by considering the small number of figurative objects discovered in the southern part of Etruria. Moreover, it is a unique find not only because of its appearance but also because of the context in which it was found, namely a place of worship, which represents an ambit in which no such statuettes have been found so far.



Fig. 2. Bronze statuette from Lake Bolsena: front (left) and back (right). Location of the sampling point.

In the last thirty years, the connections between Sardinia and the opposite coasts of the Tyrrhenian Sea in the course of Protohistory, with particular attention to the beginning of the Iron Age (10th century BCE), has been a matter of debate, especially in reference to the numerous imported materials found in both areas. The great repertoire of

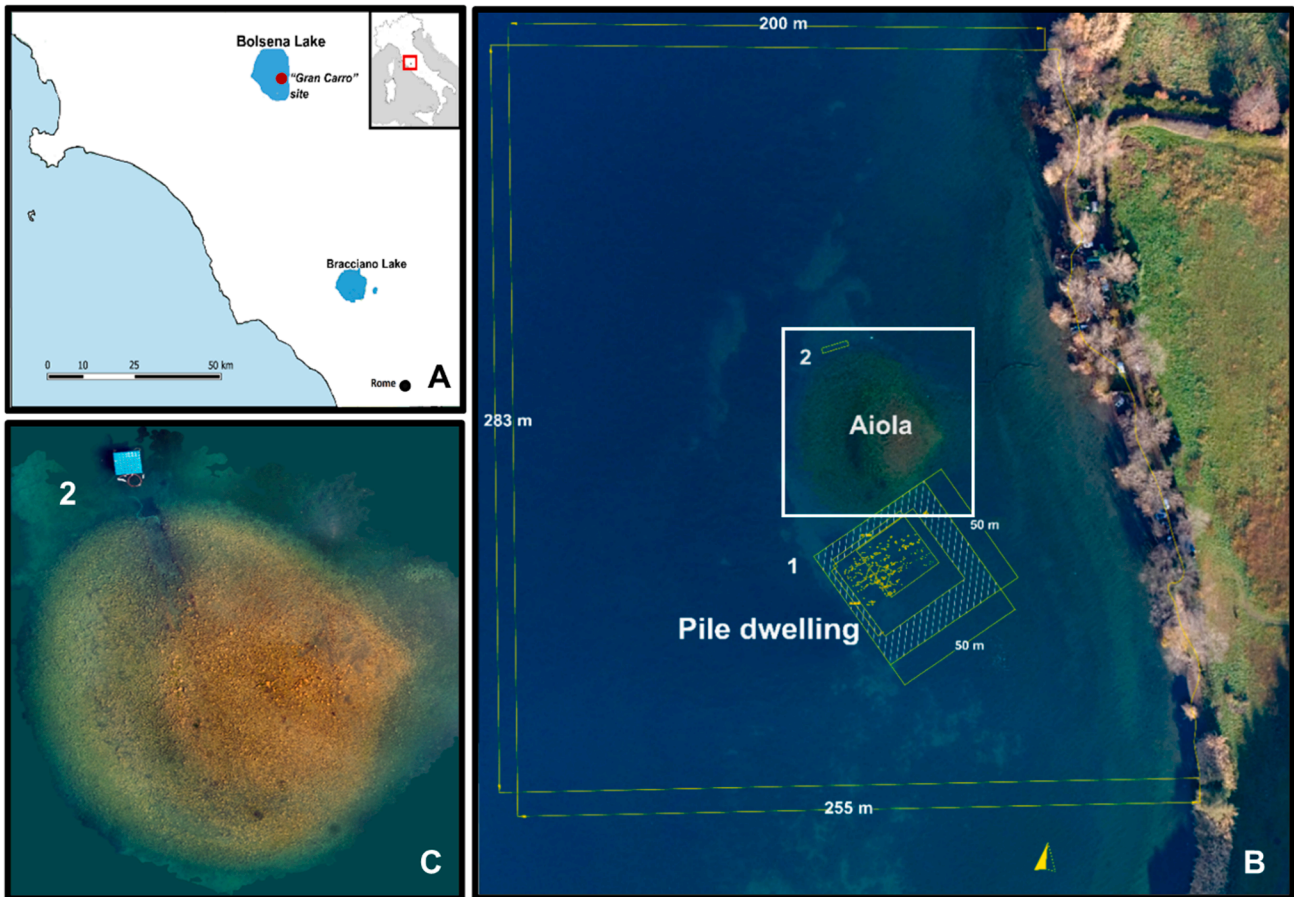


Fig. 1. A) Geographic location of Bolsena Lake. B) Archaeological site “Gran Carro” on Lake Bolsena, view from above; 1. Excavation area of the piles dwelling; 2. Aiola excavation area. C) Detail of the Aiola area (graphic processing Egidio Severi).

Sardinian artifacts found in Etruscan territory as well as that of peninsular products discovered in Sardinia - both in constant expansion - definitely indicates intense and prolonged exchanges not referable to episodic contacts (di Gennaro et al., 2023; Matta and Vandkilde, 2023; Russell and Knapp, 2017; Iaia 2017; Camporeale, 2015; Milletti 2012; Lo Schiavo et al. 2012; Arancio et al. 2010; Ialongo 2010). Therefore, the Gran Carro discovery supports new evidence corroborating previous studies suggesting intense exchange between Sardinia and mid-Tyrrhenian Italy during the Early Iron Age.

From an iconographic and stylistic point of view, it is important to note that the Gran Carro artifact does not have precise correspondences with the bronze figurines found in Sardinia, from which it differs in the presence of a horizontal cylindrical element, in the shape of a spool, resting on the head, in the filiform structure of the arms raised upwards and ending with the two disc-shaped sides of the spool, and for the bust marked by horizontal grooves. The presence of a horizontal ring on the back reinforces the hypothesis that the small sculpture was complementary to a more complex object. References to Sardinian productions can instead be the circled eyes, the straight nose combined with eyebrows in relief with a horizontal element, with a braided hairstyle, and the neck covered with a twisted thread, albeit of a very irregular and indistinct shape.

For all these reasons it is fundamental to characterize the figurine and to try to establish the provenance of the metal composing it. In this study, the sample has been fully characterized by using non-invasive surface analysis by Energy Dispersive X-Ray Fluorescence (ED-XRF) analysis integrated by Monte Carlo simulations. The results obtained by XRF were then compared and confirmed using a combination of electron beam techniques (SEM-EDS, EPMA) on a micro-fragment extracted from the object, as described in the Method section. The chemical data were then integrated by metallographic (RLOM) and isotopic (LIA) data on the same small fragment.

The compositional results obtained by non-invasive ED-XRF and Monte Carlo simulations method (Porcaro et al., 2022) and those resulting from the micro-invasive SEM-EDS and EMPA bulk analyses proved to be fully consistent.

## 2. Materials and methods

In the field of cultural heritage, the use of non-destructive techniques for investigation campaigns is essential. In this paper, as mentioned before, the preliminary characterization and quantification of the chemical elements present in the sample were determined through the combination of the X-ray fluorescence (EDXRF) and Monte Carlo simulation (MC) techniques. The results have been compared and completed by the bulk analyses of a micro-sample detached from the bottom of the statuette (Fig. 2).

The method of the ED-XRF is widely exploited in archaeometry, its advantage in addition to being non-destructive, is also that it can be portable, allowing in situ measurements. It is based on the interaction of X-rays with the matter, which allows one to determine the elemental composition of the sample examined (Silveira and Falcade, 2022; Brunetti et al., 2016a). ED-XRF is a surface technique because the information we obtain relates to a surface layer about 100–300  $\mu\text{m}$ -thick, depending on the composition and density of the surface itself. This implies that if the artifact presents a substantial alteration or patination, the results obtained will not be representative of the bulk, but only of the most superficial layer (Figueiredo et al., 2013). However, if the patina is not too thick, the fluorescence and scattered photons emitted from the bulk will be detected, and the “real” composition of the unaltered alloy can be determined by integrating the ED-XRF measure with Monte Carlo (MC) simulation according to the protocol described in Brunetti et al. (2015b). Moreover, the combination of the EDXRF technique with MC simulation enables the characterization of multilayer artefacts (Vincze et al., 1993; Brunetti et al., 2004; Golosio et al., 2014; Brunetti et al., 2015b).

In this work, an MC code, called XRM, was used that simulates the interaction of X-rays in a fast way. The MC code uses XRAYLIB, an X-ray atomic data library (Schoonjans et al., 2011). The simulation protocol requires that after modelling the experimental settings, it is necessary to provide both the composition profile and the sample structure (Brunetti et al., 2015a; Vincze et al., 1993; Schoonjans et al., 2012; Bottigli et al., 2004; Brunetti and Golosio, 2014).

The advantage of using these two techniques is that there is no need for sample preparation or removal of the corrosion patina. So, it is possible to know the composition and thickness of both the metal and the overlying layers, such as corrosive and/or protective layers.

The error in the elemental composition is mainly determined by the error in the values of the atomic parameters involved in the quantification. Moreover, the total error increases with the order of interactions used in the simulation/quantification. Here we consider interaction up to the third order, even if any order can be simulated, because the error for a higher interaction order will make the quantification values meaningless. For all these reasons an error less than 5 wt% for the main chemical elements and 10 wt% for the minor elements (>1%) can be estimated.

A portable XRF (Amptek mini-X) equipped with an X-ray tube with a rhodium anode and an SDD X-123 detector, set at 40 keV and 5–20  $\mu\text{A}$ , was used in this study. The distance between the sample and the detector was set at 2 cm. Regarding the geometry of the system it can be adapted to the geometry of the sample. Here, the detector has been placed vertically to the surface, while the X-Ray tube forms an angle of about 45° with both the surface and the line between the surface of the sample and the centre of the surface of the detector.

In a second moment, after a careful observation under a stereomicroscope, a few micro-fragments (4–5 mg) were detached from the extremity of the anthropomorphic bronze (Fig. 2) using a fine steel blade, paying attention to extract fresh metal, without oxidized portions and avoiding surface contaminations. One of the micro-samples was embedded in epoxy resin, preserving the original orientation in the object, and used to perform chemical and metallographic analysis (Scott, 2011). At first, an optical microscope with polarized reflected light was used in order to gain information about the overall micro-structure and micro-texture of the metal, that is the distribution of the different metal phases, the eventual presence and distribution of inclusions, the possible presence of leftover segregations and contaminations.

After the application of a conductive carbon coating on the cross-section, SEM-EDS analyses were performed using a COXEM EM 30AX plus instrument equipped with tungsten source (W), equipped with a solid-state detector for image acquisition of backscattered electrons (BSE), secondary electron detector (SE) and EDAX Element-C2B system (Energy Dispersive Spectroscopy) for X-ray microanalysis. All observations were performed at 20 kV, at a working distance of 12 mm and the time of count applied for EDS analysis was 100 s. The method ZAF was used for the corrections of the data. In SEM-EDS analyses the instrumental detection limit is about 0.1–0.5 % by weight and depending on the elements analysed; the analyses are always normalized, and therefore are considered semi-quantitative. The analyses were performed in area mode for statistical purposes and obtained as an average of 3 different areas of the order of 200x100  $\mu\text{m}^2$ . They are expressed as weight percentage of the elements (wt.%).

Quantitative chemical analyses of trace and minor elements in the metal matrix, inclusions and segregations were carried out using a JEOL 8200 Super Probe fitted with five vertical wavelength-dispersive spectrometers (WDS) and one energy dispersive spectrometer (EDS), housed at UNITECH laboratory, Department of Earth Sciences of Milano University. The working conditions were accelerating voltage of 15 kV and beam current intensity of 5 nA. The spot size of the beam was about 1  $\mu\text{m}^3$ . The chemical composition of the main metal phases of the sample under study was calculated as an average of 6 analysis points and is expressed in percentages by weight of elements (wt.%).

Furthermore, metallographic observations were carried out with the

aim of characterizing the metal micro-structure at the sampling point. Being a bronze artifact, the etching was carried out using an acid alcoholic solution of ferric chloride (Scott, 2011).

Finally, for the provenance study by Lead Isotopic Analysis (LIA), the second aliquot of metal detached from the statuette was pre-treated and dissolved in the ultra-clean room available at the ultraclean room installed at the Department of Geosciences, University of Padova. The micro-fragment (~2 mg) was dissolved following the same procedure described in Villa (2009), using the SrSpec™ resin (EICROM Industries) (Horwitz et al., 1992). Pb isotope measurements were run on a Neptune MC-ICPMS, housed at the CIGS - Centro Interdipartimentale Grandi Strumenti of the University of Modena and Reggio Emilia (Italy). The mass bias correction was performed with a Tl spike, and the external calibration by using the NIST SRM 981 reference material. Typical in-run relative uncertainties (2 SE of the mean) on  $^{206}\text{Pb}/^{204}\text{Pb}$ ,  $^{207}\text{Pb}/^{204}\text{Pb}$  and  $^{208}\text{Pb}/^{204}\text{Pb}$  isotope ratios were smaller than 0.02%. The measured isotopic composition for SRM 981 was indistinguishable from the certified value and the recent, more precise literature measurements (Rehkämper and Mezger, 2000), so that no adjustment of the measured ratios was necessary. The external reproducibility on the SRM 981 reference material amounted to  $\pm 0.015\%$  (2 $\sigma$ ), very similar to the individual in-run precision on unknown samples.

### 3. Results and discussion

When dealing with a submerged or a buried artifact many parameters regulate the corrosion process, such as temperature, pH, the percentage of oxygen, salt, and the composition of the sediment. The surface patina of an artifact is thus determined by various factors, both intrinsic such as the composition and microstructure, and extrinsic such as the environmental conditions in which it is found (Selwyn, 2004). The patina layer, which is generally called “noble” (Gettens, 1970; Robbiola et al., 1998), guarantees the bronze greater resistance to corrosion, as it acts as a barrier that protects it from further degradation.

The sample structure was modelled using Monte Carlo simulation, spectra were compared with different multilayer structures. The best result was obtained with a three-layer model: a protective film (Paraloid-like), on average 40  $\mu\text{m}$  thick, applied during the conservation intervention, a second very thin layer, about 8  $\mu\text{m}$ , of corrosive patina, and finally the alloy layer (Fig. 3). As previously mentioned, it is possible to know the thickness of the layers that make up a sample also thanks to the scattering phenomenon, which mainly constitutes the background of the spectrum. The thickness of the layers affects the intensity of the peaks, the greater the thickness and the density, the more this will

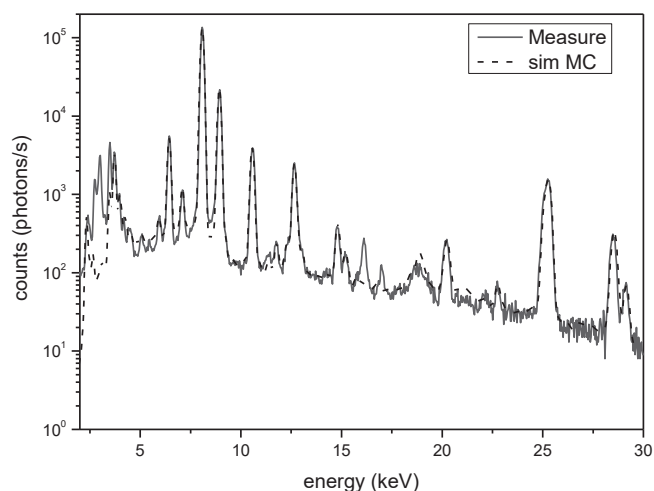


Fig. 3. Experimental (solid line) and simulated (dashed line) spectrum of the nape area.

attenuate the intensity of the peaks, especially on those at lower energies (Brunetti et al., 2016b).

Therefore, in the case of the patina or protective layers, although the light elements part (atomic numbers lower than sodium) cannot be directly identified, its presence will influence the spectrum, mainly the background part. Thus, the light element contributions to the spectrum can be modeled in the MC simulation (Bottaini et al., 2018; Cesareo et al., 2013). Of course, the light part of the corrosion patina cannot be determined/modelized with high precision, because several light elements will produce similar attenuation or because the intrinsic irregularities of this type of layer, but by considering their effect on the concentration of fluorescence producing elements (say copper, tin and lead for example) a good estimation of the composition can be obtained.

Based on the simulation results the artifact studied in this work is made of tin-bronze, whose composition is made up of 92.3 wt% of copper, 6.4 wt% of tin, and 1.2 wt% of lead. In the ED-XRF spectra, other elements have also been identified such as sulphur, calcium, manganese, iron, arsenic, silver, and iodine; their presence is due to the small portions of alteration patina (Fig. 4) occurred for the interaction of the artefact with the corrosive environment in which it was buried.

The SEM-EDS analysis of the metal section (Fig. 4a) confirms that the alloy is a tin-bronze (Sn ~ 6.6%) characterized by a small amount of Pb 0.8%, the latter is considered to be natural contamination of the mineral charge and not an intentional casting addition (analysis SEM-EDS, Table 1).

The cross-section of the sample also shows a heterogeneous  $\alpha$ -phase characterized by a marked residual coring due to variations in the Sn content falling within the range of average values 2.9–11.6%, with traces of As (0.49 wt%), Zn (0.06 wt%), Se (0.03 wt%) and Te (0.06 wt %) (EPMA analysis, in Table 2). Moreover, SEM-EDS analyses allowed to have information about the different types of inclusions and segregations present in the sample (Fig. 4b–c). In this case, sulphides of the  $\text{Cu}_2\text{S}$  type (dark gray),  $\delta$ -phase (light gray) and Pb segregations (white) were noted.

The microstructure, revealed after the chemical etching, shows small grains with twinned and slip lines inside them and flattened sulphides along a preferential orientation (Fig. 4d). These evidences indicate that the metal was subjected to several steps of hammering and annealing, probably due to smoothing and decoration after the casting process. In addition, the incomplete absorption of  $\delta$ -phase by the  $\alpha$ -phase is a further indication that annealing and alloy homogenization were not fully reached. This is not surprising, considering that the sample was extracted close to the extremity of the figurine (Fig. 2).

Finally, LIA has been performed to obtain information about the origin of the copper used for the statuette. A crucial point for a reliable identification of the origin of the metal is the interpretation of the lead isotopic data. In fact, this step is carried out by reasoned comparison with an extensive database containing both geochemical and isotopic data of mineralizations of the Mediterranean area, developed over the years by the AACP project (Alpine Archeocopper Project, 2022), and integrated by the most relevant data available in the literature (OXALID, 2018; BRETTSCHAIFE, 2022; Ling et al., 2014; Nimis et al., 2012; Nimis et al., 2017; Artioli et al., 2016; Artioli et al., 2020; García De Madina-beitia et al., 2021; Tomczyk, 2022). As previously discussed, the reliability and good results of the method have been demonstrated by several studies recently carried out both on metal finds and on ores (Nimis, 2010; Artioli et al., 2017; Canovaro et al., 2019). The values of the isotope ratios of lead determined for the findings under study are summarized in Table 3, with the error at  $\pm 2\text{SE}$ .

For the interpretation of the origin of the metal, the results obtained were preliminary processed with the Euclidean Test, which allows you to verify the minimum distance in 3D-space between the measured object (unknown) and all the data of the cupriferous mineralizations contained in the AACP database (Alpine Archeocopper Project, 2022). On the basis of the “ranking” obtained, the isotopic data of the find are therefore compared with deposits which, in addition to being

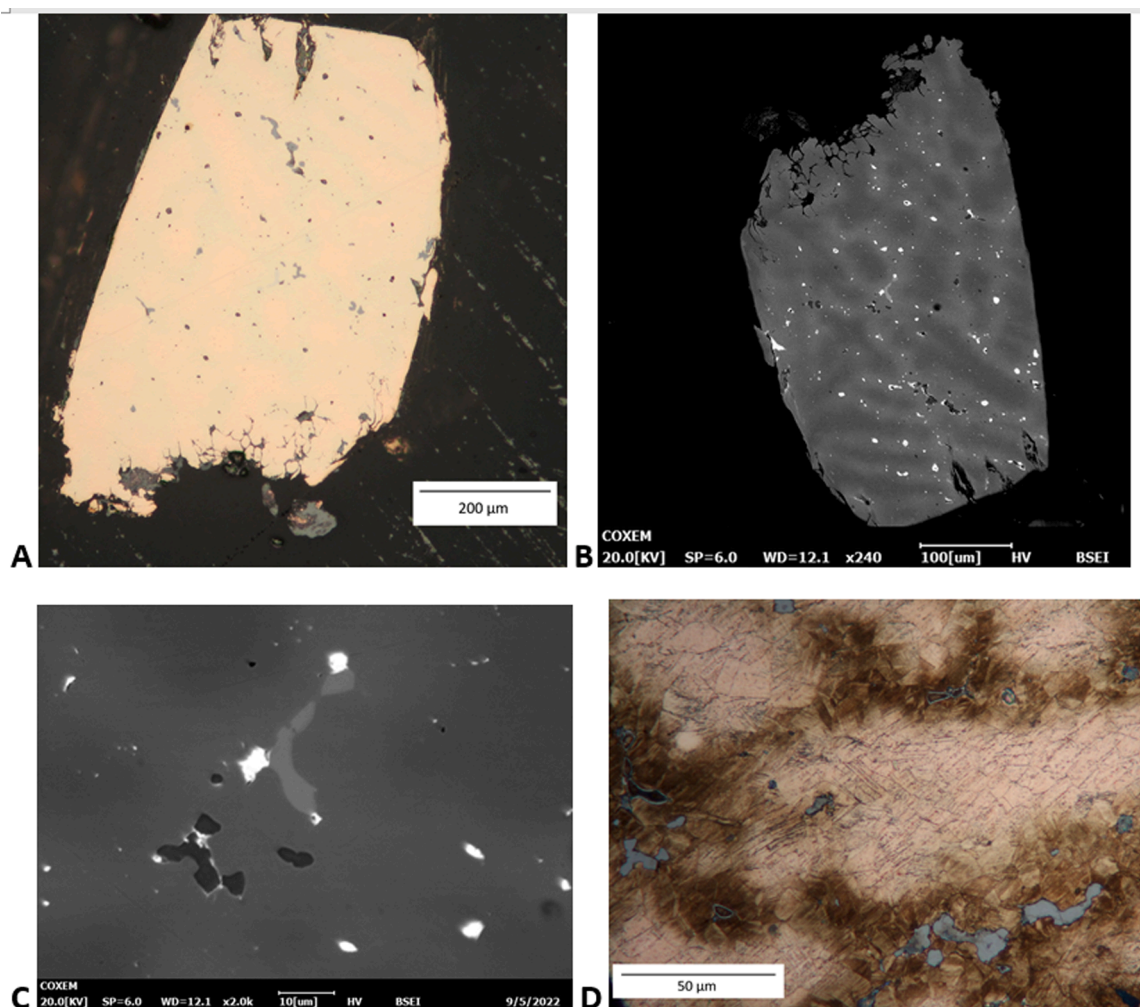


Fig. 4. a) RL-OM image showing the presence of coring (light pink) and the distribution of Cu-sulphides (gray); b) SEM-BSE image remarking the heterogeneous metal phase; c) SEM-BSE image, detail of the  $\delta$ -phase (light grey), Cu-sulphides (dark gray) and Pb (white); d) RL-OM image, after chemical etching, showing a granular structure with twins and slip lines. (For interpretation of the references to colour in this figure legend, the reader is referred to the web version of this article.)

Table 1

SEM-EDS chemical analysis (wt.%) and calculated as the average of 3 areal analyses. SD, standard deviation of the measures.

| Sample    | Cu (wt. %) | Sn (wt. %) | Pb (wt. %) | Total |
|-----------|------------|------------|------------|-------|
| Bols-Stat | 92.5       | 6.6        | 0.8        | 100.0 |
| SD        | 0.3        | 0.3        | 0.6        |       |

mathematically more probable, are also geochemically compatible with what was found during the analyses.

As seen above, the chemical analyses indicate that the artifact is made of copper smelted from sulphides, presumably from chalcopyrite, and it is characterized by some trace elements such as As and Ag. The

interpretation of the origin requires careful reflection and discussion, as isotopic ratios plot in an area with different fields overlapping, as remarked in the diagrams in Fig. 5a–b. Considering not only the geochemical aspects, but also the archaeological and relational sides, the bronze under study exhibits a Pb isotope composition compatible with the groups of ore deposits from Iglesias/Sulcis, in Sardinia. This interpretation is reinforced by the fact that in these deposits is attested the presence of arsenopyrite, compatible with the traces of As found in the alloy (Cavinato and Zuffardi, 1948; Zuffardi, 1982; Salvadori and Zuffardi, 1973; Boni and Koepfel, 1985; Moroni et al., 2019). However, it is due to the mention of a partial overlap with the Iberian area (Alcudia and Ossa Morena), where the signal refers primarily to Pb- and Zn-deposits. The fields of Tuscany are reported exclusively for comparison, but they do not show any overlap, excluding the area from the

Table 2

EPMA chemical analyses relating to the average composition of  $\alpha_1$  and  $\alpha_2$  phases (calculated as mean of 5 points analyses). SD, standard deviation of the measures. The average is arithmetic mean between Cu-rich and Cu-poor phases.

| Metal phase | S    | Cl   | Mn   | Fe   | Co   | Ni   | Cu    | Zn   | As   | Se   | Ag   | Sn    | Sb   | Te   | Pb   | Bi   | Tot    |
|-------------|------|------|------|------|------|------|-------|------|------|------|------|-------|------|------|------|------|--------|
| $\alpha_1$  | 0.01 | 0.00 | 0.03 | 0.02 | 0.03 | 0.05 | 87.74 | 0.06 | 0.75 | 0.04 | 0.08 | 11.57 | 0.00 | 0.06 | 0.15 | 0.03 | 100.61 |
| SD          | 0.01 | 0.01 | 0.03 | 0.02 | 0.03 | 0.04 | 1.24  | 0.06 | 0.3  | 0.05 | 0.03 | 1.15  | 0.00 | 0.05 | 0.23 | 0.04 |        |
| $\alpha_2$  | 0.01 | 0.00 | 0.03 | 0.01 | 0.02 | 0.02 | 97.23 | 0.06 | 0.23 | 0.02 | 0.02 | 2.89  | 0.00 | 0.05 | 0.05 | 0.08 | 100.73 |
| SD          | 0.01 | 0.00 | 0.03 | 0.01 | 0.02 | 0.05 | 0.69  | 0.06 | 0.05 | 0.02 | 0.02 | 0.58  | 0.00 | 0.05 | 0.04 | 0.06 |        |
| average     | 0.01 | 0.00 | 0.03 | 0.02 | 0.02 | 0.04 | 92.49 | 0.06 | 0.49 | 0.03 | 0.05 | 7.23  | 0.00 | 0.06 | 0.10 | 0.05 | 100.67 |

**Table 3**  
Pb isotope ratios measured on the micro-fragment of the anthropomorphic bronze.

| Label     | $^{206}\text{Pb}/^{204}\text{Pb}$ | $^{207}\text{Pb}/^{204}\text{Pb}$ | $^{208}\text{Pb}/^{204}\text{Pb}$ | $^{206}\text{Pb}/^{204}\text{Pb}$ se | $^{207}\text{Pb}/^{204}\text{Pb}$ se | $^{208}\text{Pb}/^{204}\text{Pb}$ se |
|-----------|-----------------------------------|-----------------------------------|-----------------------------------|--------------------------------------|--------------------------------------|--------------------------------------|
| Bols-Stat | 17.9732                           | 15.7034                           | 38.1370                           | 0.0010                               | 0.0008                               | 0.0020                               |

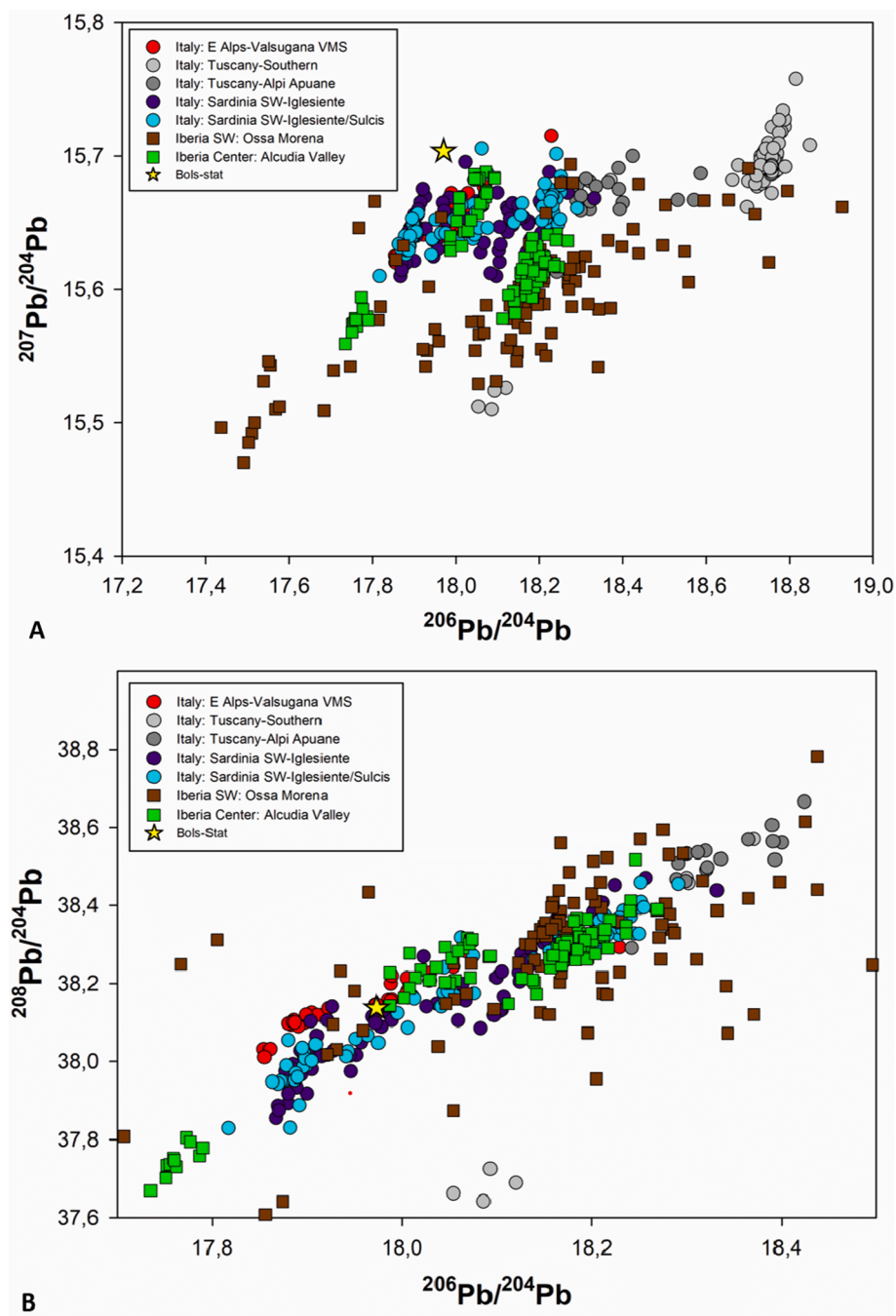


**Fig. 5.** Isotope ratio diagram a)  $^{207}\text{Pb}/^{204}\text{Pb}$  vs  $^{206}\text{Pb}/^{204}\text{Pb}$  and (b)  $^{208}\text{Pb}/^{204}\text{Pb}$  vs  $^{206}\text{Pb}/^{204}\text{Pb}$  isotopic ratios of the anthropomorphic bronze statue discovered in the Gran Carro excavation (yellow star, Bols-Stat) compared with the possible ore sources, Eastern Alps (Valsugana: [Artioli et al. 2016](#), [Nimis et al. 2012](#)), Sardinia (Iglesiente and Sulcis: [OXALID, 2018](#), [Ludwig et al. 1989](#), [Begemann et al. 2001](#), [Swainbank et al. 1982](#), [Boni and Koeppel 1985](#)), and Spain (Ossa Morena and Alcudia: [Tornos and Chiaradia 2004](#); [Hunt Ortiz, 2003](#); [Marcoux, 1998](#); [Marcoux et al. 2002](#); [Santos Zalduegui et al. 2004](#); [Santos Zalduegui et al. 2007](#); [Klein et al. 2009](#)) and Tuscany ([OXALID, 2018](#); [Lattanzi et al. 1992](#); [Chiarantini et al. 2018](#)). (For interpretation of the references to colour in this figure legend, the reader is referred to the web version of this article.)

potential ore sources. A partial overlap with Valsugana deposits is undeniable, but as suggested by [Melheim et al. \(2018\)](#) it is possible to discriminate between Sulcis Iglesiasiente and Alpine minerals in first

instance for the difference of  $^{208}\text{Pb}/^{204}\text{Pb}$  ratio ([Fig. 5](#)). Furthermore, the Gran Carro Lead Isotope  $^{207}\text{Pb}/^{204}\text{Pb}$  value appears more radiogenic and completely compatible with an extension of the Sardinian field.

#### 4. Conclusion

The study carried out on the bronze found at the archaeological site of the Gran Carro should be regarded as an important opportunity to understand the metallurgical knowledge, cultural customs and trade that took place in the Tyrrhenian Sea area in the early Iron Age.

Experimental work performed on the artifact has allowed us to characterize the metal of the object as a tin-bronze with a low Sn content. The analyses revealed the use of chalcopyrite as ore-charge for the copper extraction, associated with arsenopyrite and galena. The presence of small amounts of Pb can be considered due to the mineral charge, and for this reason the information provided by the LIA data should be referred to the copper mineral sources. The reasoned interpretation of Lead Isotope data, considering geochemical and archaeological aspects, suggests the exploitation of the Iglesias/Sulcis ore deposits, in Sardinia.

These results confirm the well-known occurrence of trade relations and cultural-social exchanges between Sardinia and southern Etruria during the Iron Age. A number of small bronze objects of Sardinian production (buttons, pendants, votive objects, models of boats, quivers, daggers etc.) have been found in several sites in Southern Etruria (Populonia, Vetulonia, Vulci, Tarquinia, Pontecagnano) starting from the second half of the 10th century BCE (overviews of imported materials, among others, in [Etruria e Sardegna 2002](#); [Milletti 2012](#)).

In the contemporary Early Iron Age necropolis of Ponte Rotto at Vulci, the presence of a tomb containing very rich grave goods including also three Sardinian bronze objects, is very indicative; in fact, the presence of a small boxing-priest bronze statuette, a basket and a stool/*tintinnabulum* in a female burial could be interpreted as the kit of a Sardinian woman married locally to an Etruscan ([Haynes, 2000](#); [Arancio et al., 2010](#)) and provides valuable chronological information for Sardinian bronzes. The finding of similar Sardinian artefacts, such as baskets ([Lo Schiavo 1994](#)), or even a bronze boat lamp in Villanovan women's burials in the Campania area ([Cerchiali et al., 2013](#)) seems to support the hypothesis that some of these materials are indicative of alliances strengthened through intermarriage between Sardinian and Villanovan groups ([di Gennaro et al., 2023](#)).

The Gran Carro find is archaeologically relevant, being the first object of Sardinian origin recovered from an early Iron Age dwelling context in Central Italy. The others come either from tombs or are without context data.

Although the provenance of copper traces back to Sulcis/Iglesiente mining areas, the question of the Gran Carro figurine manufactory appears as intricate since its stylistic characteristics and dimensions do not coincide with the iconography known for the Sardinian area.

The identification of a similar artefact among the materials traded in the antiques market, reported as originating from Sardinia and complete with a long peduncle assimilating it to a pin (<https://auctions.bertolami.com/it/lot/10503/testa-di-spillone-nuragico-in-bronzo-viii-/>), leads us to carefully evaluate whether this type could really correspond to a Sardinian production, now identified for the first time.

One cannot, however, underestimate the evidence that of the two specimens of this particular type, one was found in Etruria and the other in the illegal market - for which the stated provenance cannot be accepted without reserve - and no even partially similar specimen is to be found among the hundreds of bronze figurines from Sardinia. Thus, a double problem arises: on the one hand the possibility that it is a peninsular production made from Sardinian raw material and, on the other, that it is a fully original Sardinian artifact outside the standards known so far.

The presence of Sardinian materials in the Etruscan area would bring us back to the sphere of the rich contacts that communities on opposite sides of the Tyrrhenian activated with particular intensity in the Early Iron Age.

As known, imports from Sardinia concerned very significantly bronze artefacts, including buttons, pendants and miniaturistic objects,

boat-shape lamps, which are accompanied by the export of peculiar ceramic shapes such as jugs askoids, for which local imitations are also documented by archaeometric analyses ([Cygielman and Pagnini, 2002](#); [Delpino 2002](#)). In addition to Etruria, from Volterra to Cerveteri and with a high density around Vetulonia ([Milletti 2012](#)), the widespread presence of askoid jugs is also found in Lipari ([Cavalier and Depalmas, 2008](#)), in Sicily ([Lo Schiavo 2005](#)), in Crete ([Ferrarese Ceruti 1991](#)), in Tunisia ([Ben, 2018](#)), in the Iberian Peninsula ([Fundoni 2021](#)).

Additionally, the presence of Cypriot-made copper oxhide ingots in Sardinia testifies the wide-ranging network of Sardinian trades in the period ([Sabatini and Lo Schiavo, 2020](#)). The massive presence of Cypriot copper in the form of oxide ingots appears rather problematic precisely because of the fact that Sardinia is an island that not only possesses minerals rich in Pb, Zn and Ag (due to argentiferous galena) but also has significant copper resources.

Definitely, this is a highly-debated topic about the attestations of oxhide ingots in Sardinia (the issue is discussed in many works including [Lo Schiavo et al. 2009](#); [Sabatini 2016](#); [Kassianidou 2021](#)). In fact, although the literature refers to a representation on a sherd from a level attributed to the Middle Bronze Age and to fragments of ingots from a context of the Recent Bronze Age, in both cases these interpretations are very problematic and absolutely not resolute in terms of chronology. In this sense, it is well known that, when coupled by contextual data, the discovery sites are instead pertinent to the final phase of the Bronze Age and, more often, to the Early Iron Age ([Depalmas 2020](#): 352); therefore, in contemporary times with those of the maximum intensity of exchanges between Sardinia and the rest of the Mediterranean.

Evidently this constitutes a problematic aspect that raises further questions about the circulation of these artefacts in the West Mediterranean, both in terms of the areas involved and, above all, the timescale.

Further, this work confirms the effectiveness of non-destructive techniques such as EDXRF combined with MC simulation, which enabled the characterization of the alloy both at the level of composition and structure, coming very close to the results obtained with micro-invasive techniques, which cannot always be practiced in the field of cultural heritage.

#### Declaration of Competing Interest

The authors declare that they have no known competing financial interests or personal relationships that could have appeared to influence the work reported in this paper.

#### Data availability

Data will be made available on request.

#### References

- Alpine Archeocopper Project, [http://geo.geoscienze.unipd.it/aacp/welcome.html](http://geo.geosciienze.unipd.it/aacp/welcome.html) (accessed 23 January 2022).
- Arancio, L., Moretti Sgubini, A.M., Pellegrini, E., 2010. Corredi funerari femminili di rango a vulci nella prima età del ferro. In *Negrone Catacchio 2010*, 169–214.
- Artioli, G., Angelini, I., Nimis, P., Villa, I.M., 2016. A lead-isotope database of copper ores from the southeastern alps: A tool for the investigation of prehistoric copper metallurgy. *J. Archaeol. Sci.* 75, 27–39. <https://doi.org/10.1016/j.jas.2016.09.005>.
- Artioli, G., Angelini, I., Kaufmann, G., Canovaro, C., Dal Sasso, G., Villa, I.M., 2017. Long-distance connections in the copper age: New evidence from the alpine iceman's copper axe. *PLoS One* 12, e0179263.
- Artioli, G., Canovaro, C., Nimis, P., Angelini, I., 2020. LIA of prehistoric metals in the central mediterranean area: a review. *Archaeometry*. <https://doi.org/10.1111/arcm.12542>.
- Barbaro, B., Severi, E., 2020. L'abitato sommerso della prima età del Ferro del "Gran Carro" di Bolsena: verso una nuova prospettiva, «*Analysis Archaeologica 2018*» 4, pp. 25-51, 293-298.
- Barbaro, B., 2021. L'abitato protostorico del «Gran Carro» di Bolsena: un complesso insediativo e culturale di lunga durata sulle rive del lago. Rapporto preliminare sulle indagini 2020-2021, in *Archaeologia Marittima Mediterranea* 18, pp. 13-34.
- Begemann, F., Schmitt-Strecker, S., Pernicka, E., Lo Schiavo, F., 2001. Chemical composition and lead isotopy of copper and bronze from nuragic Sardinia. *Eur. J. Archaeol.* 4 (1), 43–85.

- Ben, J.I., 2018. La céramique sarde trouvée à utique: quelle signification? *Rivista di Studi Fenici* 45–2017, 177–198.
- Boni, M., Koepfel, V., 1985. Ore-lead isotope pattern from the Inglesiente-Sulcis area (SW sardinia) and the problem of remobilization of metals. *Miner. Deposita* 20, 185–193.
- Bottaini, C.E., Brunetti, A., Montero-Ruiz, I., Valera, A., Candeias, A., Mirão, J., 2018. Use of monte carlo simulation as a tool for the nondestructive energy dispersive x-ray fluorescence (ED-XRF) spectroscopy analysis of archaeological Copper-Based artifacts from the chalcolithic site of perdigões, southern portugal. *Appl. Spectrosc.* 72, 17–27. <https://doi.org/10.1177/0003702817721934>.
- Bottigli, U., Brunetti, A., Golosio, B., Oliva, P., Stumbo, S., Vincze, L., Randaccio, P., Bleu, P., Simionovici, A., Somogyi, A., 2004. Voxel-based monte carlo simulation of x-ray imaging and spectroscopy experiments. *Spectrochim. Acta Part B At. Spectrosc.* 59, 1747–1754. <https://doi.org/10.1016/j.sab.2004.03.016>.
- BRETTSCAIFE, <https://www.brettscaife.net/lead/data/index.html> (accessed 14 November 2022).
- Brunetti, A., Fabian, J., La Torre, C.W., Schiavon, N., 2016a. A combined XRF/Monte carlo simulation study of multilayered peruvian metal artifacts from the tomb of the priestess of chornancap. *Appl. Phys. A* 122, 571. <https://doi.org/10.1007/s00339-016-0096-6>.
- Brunetti, A., Golosio, B., 2014. A new Monte Carlo code for simulation of the effect of irregular surfaces on x-ray spectra. *Spectrochim. Acta Part B At. Spectrosc.* 94, 58–62. <https://doi.org/10.1016/j.sab.2014.03.007>.
- Brunetti, A., Sanchez del Rio, M., Golosio, B., Simionovici, A., Somogyi, A., 2004. A library for x-ray-matter interaction cross sections for X-ray fluorescence applications. *Spectrochim. Acta Part B At. Spectrosc.* 59, 1725–1731. <https://doi.org/10.1016/j.sab.2004.03.014>.
- Brunetti, A., Golosio, B., Melis, M.G., Mura, S., 2015a. A high-quality multilayer structure characterization method based on x-ray fluorescence and monte carlo simulation. *Appl. Phys. A* 118, 497–504. <https://doi.org/10.1007/s00339-014-8838-9>.
- Brunetti, A., Golosio, B., Schoonjans, T., Oliva, P., 2015b. Use of monte carlo simulations for cultural heritage x-ray fluorescence analysis. *Spectrochim. Acta Part B At. Spectrosc.* 108, 15–20. <https://doi.org/10.1016/j.sab.2015.03.014>.
- Brunetti, A., Depalmas, A., Di Gennaro, F., Serges, A., Schiavon, N., 2016b. X-ray fluorescence spectroscopy and monte carlo characterization of a unique nuragic artifact (Sardinia, Italy). *Spectrochim. Acta B At. Spectrosc.* 121, 18–21. <https://doi.org/10.1016/j.sab.2016.04.007>.
- Camporeale, G., 2015. Dalla Sardegna a Vetulonia nelle età villanoviana e orientalizzante, in Minoja M., Salis G., Usai L., a cura di, *L'isola delle torri*, Sassari, 167–173.
- Canovaro, C., Angelini, I., Artioli, G., Nimis, P., Borgna, E., 2019. Metal flow in the late bronze age across the Friuli-Venezia Giulia plain (Italy): New insights on Cervignano and Muscoli hoards by chemical and isotopic investigations. *Archaeological and Anthropological Sciences*, 11, 4829–4846. [Doi: 10.1007/s12520-019-00827-2](https://doi.org/10.1007/s12520-019-00827-2).
- Cavalier, M., Depalmas, A., 2008. *Materiali sardi nel villaggio di lipari. I frammenti ceramici e le correlazioni*, *Rivista di Scienze Preistoriche* LVIII, pp. 281–300.
- Cavinato, A., Zuffardi, P., 1948. In: *Notizie sull'industria del piombo e dello zinco in Italia*. P.Z., Milano, Montevecchio, S.I.
- Cerchiai, L., d'Agostino, B., Pellegrino, C., Tronchetti, C., Parasole, M., Bondioli, L., Sperduti, A., 2012–13. Monte Vetrano (Salerno) tra Oriente e Occidente a proposito delle tombe 74 e 111, *AION. Annali di Archeologia e Storia Antica* 2012–2013, 73–108.
- Cesareo, R., De Assis, J.T., Roldàn, C., Bustamante, A.D., Brunetti, A., Schiavon, N., 2013. Multilayered samples reconstructed by measuring ka/Kb or la/Lb x-Ray intensity ratios by EDXRF. *Nucl. Instr. Methods Phys. Res. B* 312, 15–22. <https://doi.org/10.1016/j.nimb.2013.06.019>.
- Chiarantini, L., Benvenuti, M., Costagliola, P., Dini, A., Firmati, M., Guideri, S., Villa, I. M., Corretti, A., 2018. Copper metallurgy in ancient Etruria (southern tuscany, Italy) at the Bronze-Iron age transition: a lead isotope provenance study. *J. Archaeol. Sci. Rep.* 19, 11–23. <https://doi.org/10.1016/j.jasrep.2018.02.005>.
- Cygielman, M., Pagnini, L., 2002. Presenze sarde a vetulonia: alcune considerazioni. *Etruria e Sardegna* 2002, 387–410.
- Delpino, F., 2002. *Brocchette a collo obliquo dell'area etrusca. Etruria e Sardegna* 2002, 363–386.
- Depalmas, A., 2020. *trasmissione di manufatti, modelli e tecniche tra la sardegna e il mediterraneo orientale. Rivista di Scienze Preistoriche* LXX S1–2020, 345–356.
- di Gennaro, F.; Amicone, S.; D'Orlando, R.; Mancini, P., 2023. *L'insediamento villanoviano dell'isola di Tavolara presso le coste della Gallura*, *FastiOnlineDocuments&Research*.
- Etruria e Sardegna 2002. *Etruria e Sardegna centro-settentrionale tra l'età del bronzo finale e l'arcaismo*, *Atti del XXI Convegno di Studi Etruschi ed Italici (Sassari-Alghero-Oristano-Torralba, 13-17 ottobre 1998)*, Pisa – Rom.
- Ferrarese Ceruti, M.L., 1991. *Creta e Sardegna in età postmicenea*, Una nota, in *La transizione dal Miceneo all'Alto Arcaismo*, dal palazzo alla città, *Monografie scientifiche, Serie Scienze Umane e sociali*. Roma, 587–591.
- Figueiredo, E., Araújo, M.F., Silva, R.J., Vilaça, R., 2013. Characterisation of a proto-historical bronze collection by micro-EDXRF. *Nucl. Instrum. Methods Phys. Res. Sect. B Beam Interact. Mater. Atoms* 296, 26–31. <https://doi.org/10.1016/j.nimb.2012.11.019>.
- Fioravanti, A.; Camerini, E., 1977. *L'abitato villanoviano del Gran Carro sommerso nel Lago di Bolsena (1959-1977)* (Roma 1977).
- Fundoni, G., 2021. *Le relazioni tra la Sardegna e la penisola iberica tra la fine del II e i primi secoli del I millennio a.C.*, *Nesoi/Isle/Islands. Ricerche, contesti, problemi di Protostoria del Mediterraneo*, 2, Roma.
- García De Madinabeitia, S., Gil Ibarra, J.I., Santos Zalduegui, J.F., 2021. IBERLID: A lead isotope database and tool for metal provenance and ore deposits research IBERLID: A lead isotope database and tool for metal provenance and ore deposits research. *Ore Geol. Rev.* <https://doi.org/10.1016/j.oregeorev.2021.104279>.
- Getters, R.J., 1970. *Patina noble and vile*. In: *Doehringer, S., Mitten, D.G., Steinberg, A. (Eds.), art and Technology: a Symposium on Classical Bronzes*. MIT Press, Cambridge, MA, pp. 57–72.
- Golosio, B., Schoonjans, T., Brunetti, A., Oliva, P., Masala, G.L., 2014. Monte carlo simulation of x-ray imaging and spectroscopy experiments using quadric geometry and variance reduction techniques. *Comput. Phys. Commun.* 185, 1044–1052. <https://doi.org/10.1016/j.cpc.2013.10.034>.
- Gonzalez, R.A., 2012. *Sardinian bronze figurines in their mediterranean setting*. *Prähistorische Zeitschrift* 87 (1), 83–109.
- Haynes, S., 2000. *Etruscan civilization: a cultural history*. The J. Paul Getty Museum, Los Angeles, pp. 18–20.
- Horwitz, E.P., Chiarizia, R., Dietz, M.L., 1992. A novel strontium-selective extraction chromatographic resin; solvent Extr. *Ion Exch.* 10, 313–336. <https://doi.org/10.1080/07366299208918107>.
- Hunt Ortiz, M., 2003. *Isotopic characterization of the south west iberian peninsula. Prehistoric mining and metallurgy in South West Iberian Peninsula*, Oxford, Archaeopress 218–258. <https://doi.org/10.30861/9781841715544>.
- Iaia, C., 2017. *External relationship (10th cent.-730 BCE)*, in Naso, A. (ed.), *Etruscology*, chapter 44.
- Ialongo, N., 2010. *Ripostigli e complessi di bronzi votivi della sardegna nuragica tra bronzo recente e prima età del ferro*. *Origini XXXII* 315–352.
- Kassianidou, V., 2021. *Oxhide Ingots 2020*. *New Research*. In: Perra, M., Lo Schiavo, F. eds. *Cultural Contacts and Trade in Nuragic Sardinia: The Southern Route (Sardinia, Sicily, Crete And Cyprus)* Proceedings of the Fourth Festival of the Nuragic Civilization (Orroli, Cagliari). Cagliari: Arkadia, 109–126.
- Klein, S., Domergue, C., Lahaye, Y., Brey, G.P., von Kaenel, H.-M., 2009. *the lead and copper isotopic composition of copper ores from the sierra morena (Spain)*. *J. Iber. Geol.* 35 (1), 59–68.
- Lattanzi, P., Hansmann, W., Koepfel, V., Costagliola, P., 1992. *Source of metals in metamorphic ore-forming processes in the apuane alps (NW tuscany, Italy): Constraints by pb-isotope data*. *Mineral. Petrol.* 45, 217–229. <https://doi.org/10.1007/BF01163113>.
- Lilliu, G., 1966. *Sculture della Sardegna nuragica*, Verona.
- Ling, J.; Stos-Gale, Z.; Grandin, L.; Billström, K.; Hjärthner-Holdar, E.; Persson, P. O., 2014. *Moving metals II: Provenancing Scandinavian bronze age artefacts by lead isotope and elemental analyses*, *Journal of Archaeological Science*, 41, 106–132. [Doi: 10.1016/j.jas.2013.07.018](https://doi.org/10.1016/j.jas.2013.07.018).
- Lo Schiavo, F., 1994. *Bronzi nuragici nelle tombe della prima età del ferro di pontecagnano*. In: *La Presenza Etrusca Nella Campania Meridionale. Atti delle giornate di studio*, Firenze, pp. 61–82.
- Lo Schiavo, F.; Milletti, M.; Rafanelli, S.; Bernardini, P.; Zucca, R., 2012. *Navi di bronzo dai santuari nuragici ai tumuli etruschi di Vetulonia*, *Sardegna Archeologica* 1, Sassari.
- Lo Schiavo, F., Muhly, J., Maddin, R., Giunlia-Mair, A. (Eds.), 2009. *the Oxhide ingots in the Central Mediterranean*. ICEVO-CNR, Rome.
- Lo Schiavo, F., 2005. *Le brocchette askoidi nuragiche nel Mediterraneo all'alba della storia in Sicilia Archeologica*, 101–116.
- Ludwig, K.R., Vollmer, R., Turi, B., Simmons, K.R., Perna, G., 1989. *Isotopic constraints on the genesis of base-metal ores in southern and central sardinia*. *Eur. J. Mineral.* 1, 657–666.
- Marcoux, E., 1998. *Lead isotope systematics of the giant massive sulphide deposits in the iberian pyrite belt*. *Miner. Deposita* 33, 45–58. <https://doi.org/10.1007/s001260050132>.
- Marcoux, E., Pascual, E., Onézime, J., 2002. *Hydrothermalisme anté-Hercynien en Sud-ibérie: apport de la géochimie isotopique du plomb*. *C. R. Geoscience* 334, 259–265. [https://doi.org/10.1016/S1631-0713\(02\)01734-0](https://doi.org/10.1016/S1631-0713(02)01734-0).
- Matta, V., Vandkilde, H., 2023. *the state of the debate: Nuragic metal trade*. *Open Arch.* 9, 20220280.
- Melheim, L., Grandin, L., Persson, P.-O., Billström, K., 2018. *Moving metals III: Possible origins for copper in bronze age denmark based on lead isotopes and geochemistry*. *JAS* 96, 85–105.
- Milletti, M., 2012. *Cimeli d'identità. Tra Etruria e Sardegna nella prima età del ferro*, Roma.
- Moravetti, A.; Alba, E.; Foddai L. (a cura di), 2014. *La Sardegna nuragica. Storia e materiali*, Carlo Delfino editore, Sassari 2014, pp. 347–404.
- Moroni, M., Rossetti, P., Naitza, S., Magnani, L., Ruggieri, G., Aquino, A., Tartarotti, P., Franklin, A., Ferrari, E., Castelli, D., Oggiano, G., Secchi, F., 2019. *Factors controlling hydrothermal nickel and cobalt mineralization – Some suggestions from historical ore deposits in Italy*. *Minerals* 9, 429.
- Nimis, P., Omenetto, P., Giunti, I., Artioli, G., Angelini, I., 2012. *Lead isotope systematics in hydrothermal sulphide deposits from the central-eastern southalpine (northern Italy)*. *Eur. J. Mineral.* 24, 23–37. <https://doi.org/10.1127/0935-1221/2012/0024-2163>.
- Nimis, P., Omenetto, P., Stasi, G., Canovaro, C., Dal Sasso, G., Artioli, G., Angelini, I., 2017. *Lead isotope systematics in ophiolite-associated sulphide deposits from the western alps and northern apennine (Italy)*. *Eur. J. Mineral.* 30, 17–31. <https://doi.org/10.1127/ejm/2018/0030-2696>.
- Nimis, P., 2010. *Some remarks on the use of geochemical tracers for metal provenancing, in Late Roman Glazed pottery in Carlinio and in Central-East Europe*, Oxford: BA., Magrini C, Ed., 3–9.
- OXALID, *Oxford archaeological lead isotope database*. <http://oxalid.arch.ox.ac.uk> (accessed 27 August 2018).

- Porcaro, M., Depalmas, A., Lins, S., Bulla, C., Pischedda, M., Brunetti, A., 2022. Nuragic working tools characterization with corrosion layer determinations, *Materials*, in press.
- Rehkämper, M., Mezger, K., 2000. Investigation of matrix effects for Pb isotope ratio measurements by multiple collector ICP-MS: verification and application of optimized analytical protocols. *J Anal Atom Spectrom* 15, 1451–1460. <https://doi.org/10.1039/b005262k>.
- Robbiola, L., Blengino, J.-M., Fiaud, C., 1998. Morphology and mechanisms of formation of natural patinas on archaeological Cu-Sn alloys. *Corros. Sci.* 40, 2083–2111. [https://doi.org/10.1016/S0010-938X\(98\)00096-1](https://doi.org/10.1016/S0010-938X(98)00096-1).
- Russell, A., Knapp, B., 2017. Sardinia and Cyprus: An alternative view on cyprites in the central mediterranean. *PBSR* 85, 1–35.
- Sabatini, S., 2016. Revisiting late bronze age copper oxhide ingots: Meanings, questions and perspectives. In: Aslaksen, O.C. (Ed.), *Local and Global perspectives on Mobility in the Eastern Mediterranean*. Norwegian Institute in Athens, Athens, pp. 15–62.
- Salvadori, I., Zuffardi, P., 1973. In: *Itinerari geologici, mineralogici, giacimentologici in Sardegna – Vol I*. Ente Minerario Sardo, Cagliari, 29–46.
- Santos Zalduegui, J.F.; García de Madinabeitia, S.; Gil Ibarra, J.I.; Palero, F., 2004. A lead isotope database: The Los Pedroches - Alcudia area (Spain); Implications for archaeometallurgical connections across southwestern and southeastern Iberia, *Archaeometry*, 46 (4), pp. 625–634. [Doi: 10.1111/j.1475-4754.2004.00178.x](https://doi.org/10.1111/j.1475-4754.2004.00178.x).
- Sabatini, S., Lo Schiavo, F., 2020. Late bronze age metal exploitation and trade: Sardinia and Cyprus. *Mater. Manuf. Process.* 35 (13), 1501–1518. <https://doi.org/10.1080/10426914.2020.1758329>.
- Santos Zalduegui, J.F., Guinea, A., Ábalos, B., Gil Ibarra, J.I., 2007. Composición isotópica del pb en galenas de la región de la falla de azuaga. *Aportaciones al modelo plumbotectónico de la Zona de Ossa-Morena*, *Geogaceta* 43, 7–10.
- Schoonjans, T., Brunetti, A., Golosio, B., Sanchez del Rio, M., Solé, V.A., Ferrero, C., Vincze, L., 2011. The xraylib library for x-ray-matter interactions. Recent developments. *Spectrochim. Acta Part B At. Spectrosc.* 66, 776–784. <https://doi.org/10.1016/j.sab.2011.09.011>.
- Schoonjans, T., Vincze, L., Solé, V.A., Sanchez del Rio, M., Brondeel, P., Silversmit, G., Appel, K., Ferrero, C., 2012. A general monte carlo simulation of energy dispersive x-ray fluorescence spectrometers—Part 5: Polarized radiation, stratified samples, cascade effects, m-lines. *Spectrochim. Acta Part B At. Spectrosc.* 70, 10–23. <https://doi.org/10.1016/j.sab.2012.03.011>.
- Scott, D. A., 2011. *Ancient Metals: Microstructure and Metallurgy*.
- Selwyn, L., 2004. *Metals and corrosion—A handbook for the conservation professional*. Ottawa, Canada, Canadian Conservation Institute.
- Silveira, P.; Falcade, T., 2022. Applications of energy dispersive X-ray fluorescence technique in metallic cultural heritage studies, *Journal of Cultural Heritage*, Volume 57, 243–255. [Doi: 10.1016/j.culher.2022.09.008](https://doi.org/10.1016/j.culher.2022.09.008).
- Swainbank, I.G., Shepherd, T.J., Caboi, R., Massoli-Novelli, R., 1982. Lead isotopic composition of some galena ores from Sardinia. *Periodico di mineralogia* 51, 275–286.
- Tamburini, P., 1995. Un abitato villanoviano per ilacustre. Il “Gran Carro” sul Lago di Bolsena (1959–1985), *Archaeologica* 113, Tyrrhenica 5 (Roma 1995).
- Tomczyk, C., 2022. A database of lead isotopic signatures of copper and lead ores for europe and the near east. *J. Archaeol. Sci.* 146, 105657 <https://doi.org/10.1016/j.jas.2022.105657>.
- Tornos, F., Chiaradia, M., 2004. Plumbotectonic evolution of the ossa morena zone, Iberian Peninsula: Tracing the influence of Mantle-Crust interaction in Ore-Forming processes. *Econ. Geol.* 99, 965–985. <https://doi.org/10.2113/gsecongeo.99.5.965>.
- Trucco, F., 2006. Considerazioni sul rituale funerario in etruscia meridionale all’inizio dell’età del ferro alla luce delle nuove ricerche a tarquinia, in *La ritualità funeraria tra età del ferro e orientalizzante in italia* (Atti del convegno di verucchio, 26–27 giugno 2002). Pisa - Roma 95–102.
- Villa, I.M., 2009. Lead isotopic measurements in archeological objects. *Archaeol. Anthropol. Sci.* 1, 149–153. <https://doi.org/10.1007/s12520-009-0012-5>.
- Vincze, L., Janssen, K., Adams, F., 1993. A general monte carlo simulation of energy-dispersive X-ray fluorescence spectrometers—I: unpolarized radiation, homogeneous samples. *X-Ray Spectrom.* 48, 553–573. [https://doi.org/10.1016/0584-8547\(93\)80060-8](https://doi.org/10.1016/0584-8547(93)80060-8).
- Zuffardi, P., 1982. In: *Giacimentologia e Prospezione mineraria*. Pitagora Ed., Bologna, 120–132.